Journal of the European Ceramic Society **19** (1999) 451–455
© 1999 Elsevier Science Limited
Printed in Great Britain. All rights reserved
PII: S0955-2219(98)00216-7
0955-2219/99/$—see front matter

Effect of Residual Microstresses at Crystalline Multigrain Junctions on the Toughness of Silicon Nitride

Giuseppe Pezzotti[a]* and Hans-Joachim Kleebe[b]

[a]Department of Materials, Kyoto Institute of Technology, Matsugasaki, Kyoto, Japan
[b]University of Bayreuth, Materials Research Institute, D-95440, Bayreuth, Germany

(Received 26 June 1998; accepted 15 August 1998)

Abstract

Two Si_3N_4 materials with either tensile or compressive residual microstresses localized at triple-grain junctions have been analyzed with respect to their fracture behavior and microstructural characteristics. Residual tensile stresses at triple pockets were obtained, upon addition of Sc_2O_3, by initiating the crystallization of $Sc_2Si_2O_7$ with a negative volume change. On the other hand, compressive microstresses localized at triple-grain junctions were induced by adding fine ZrO_2 particles to the Si_3N_4 material, which underwent martensitic transformation upon cooling with a positive volume change. The presence of these highly localized stress fields has been shown to actually be the critical factor in determining the fracture mode of Si_3N_4 materials and, accordingly, their respective fracture toughness. In particular, tensile stress fields at triple-grain pockets can trigger debonding and splitting of the crack tip at the interface and, therefore, may provide a precursor effect for elastic bridging in the crack wake. © 1999 Elsevier Science Limited. All rights reserved

Keywords: Si_3N_4, toughness, microstructure-final, residual stress, ZrO_2.

1 Introduction

The fracture toughness of silicon nitride (Si_3N_4) ceramics has been the object of intensive research since it was shown that the toughness can be appreciably influenced by both the size and the morphology (i.e. the aspect ratio) of the Si_3N_4 grains.[1,2] The presence of columnar crystallites with large diameter in the microstructure enables the occurrence of an elastic crack bridging mechanism which can be effectively exploited in the neighborhood behind the crack tip. As a result, a steeply rising *R*-curve behavior can be achieved in the material with remarkable toughness values of $\approx 10\,\mathrm{MPa\ m^{1/2}}$ after the first $100\,\mu\mathrm{m}$ of crack extension.[3,4] Recently, fracture experiments were conducted *in situ* by Pezzotti *et al.*[5] in a toughened Si_3N_4 ceramic and, concurrently, local measurements by Raman spectroscopy of shielding/bridging tractions by elongated grains were performed. Remarkable closure stresses up to $\approx 1\,\mathrm{GPa}$ were found in unbroken columnar Si_3N_4 grains which were bridging the crack faces in elastic fashion. By observing *in situ* crack propagation, the bridging phenomenon appeared to develop according to the characteristic sequence depicted in the draft of Fig. 1. With the crack approaching a grain with a columnar shape, local debonding occurred first along the interface of the acicular grain, while the grain was also circumvented by the main crack path [Fig. 1(a) and (b)]. This process leads to the formation of an unbroken ligament (i.e. a bridging site) just behind the crack tip. After eventually observing a portion of reverse crack propagation along the crack profile [cf. Figure 1(c)], the process finally results in the development of an elastic bridging site composed of an individual columnar Si_3N_4 grain.

Although the mechanics of the formation of bridging sites can be envisaged according to the aforementioned *in situ* microscopy and quantified in terms of bridging microstresses by spectroscopy measurements,[5] a topic which remains yet to be clarified is the reason why debonding occurs in some Si_3N_4 materials rather than in others, despite the presence of similar morphological characteristics of

*To whom correspondence should be addressed. Fax: +81-75-724-7580; e-mail: pezzotti@chem.kit.ac.jp

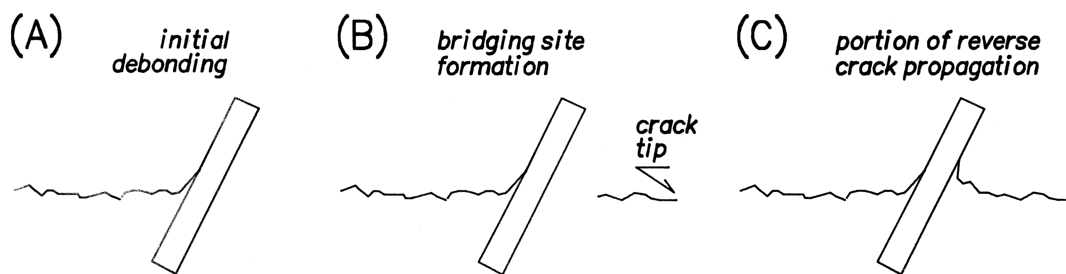

Fig. 1. Schematic of the formation of an elastic bridging site in Si_3N_4 materials containing elongated grains. Three successive phases are shown which, since the initial debonding process has occurred, lead to an elastic bridge formation.

the bulk grains. In other words, it is important to understand by which (precursor) mechanism the crack tip is allowed to locally kink into the interface rather than to cut the columnar Si_3N_4 grain, namely the potential elastic bridging site. Clearly, a number of micromechanical factors can be involved in the preliminar debonding process, a necessary condition for the occurrence of elastic bridging. For example, the magnitude of the grain diameter[1,2] as well as the intrinsic fracture energy of the glassy interface[6] are considered to be important parameters. However, the latter parameter is not supposed to vary by orders of magnitude since the fracture energy of bulk glass is hardly altered in such a pronounced way by simply modifying its chemical composition. Regarding the former parameter, it was reported earlier that Si_3N_4 materials with similar grain morphology can show very different toughening behaviors.[7] This would imply that at least another important parameter is involved in the toughening behavior of the material, which triggers the local mechanism allowing for interface debonding. Local residual stresses stored at the glass/grain interface, as a consequence of a difference in thermal expansion coefficient between the intergranular phase and the Si_3N_4 grains, have then been considered as the main reason for the crack to debond along the interface with the consequence of the formation of bridging sites.[8]

In this paper, we have analyzed by transmission electron microscopy (TEM) the crack profile of two Si_3N_4 materials, in which local stresses of high magnitude were localized at the triple pockets, however, with opposite sign. High tensile stresses were obtained by exploiting the negative volume change related to the crystallization process of a Sc_2O_3 containing glass phase. On the other hand, highly localized compressive stresses could be produced at grain boundaries by introducing fine ZrO_2 particles into the Si_3N_4 microstructure, which martensitically transformed upon cooling from processing temperature, with a positive volume change. The effect of these two opposite microscopic stress fields on the local crack path is analyzed and discussed in the following.

2 Experimental procedure

The two Si_3N_4 materials studied were processed by adding 5 wt% Sc_2O_3 and 1·5 wt% Al_2O_3 + 2·7 wt% ZrO_2, acting as sintering aids, respectively. These specific materials were selected among others, because they represent two enlightening examples regarding the present topic of residual stresses at triple pockets. The salient informations on material processing and characterization procedures are given hereafter. Blends of Si_3N_4 and the added metal oxide powders were processed in butanol and subsequently dried and granulated. Ball milling with Si_3N_4 milling balls and container was employed to obtain an intimate mixing of the starting powders. A gas-pressure sintering cycle with a maximum pressure of 10 MPa N_2 and a maximum temperature of 1925°C held for 1 h was adopted for densifying both materials (relative density >99%). A Leica Quantimet 500 image processing system was utilized for quantitative analysis of the overall microstructures, using scanning electron microscopy (SEM) images of plasma-etched cross sections, with respect to both average grain diameter, d, and apparent aspect ratio, R. Image processing was carried out on a total sampling surface of $\approx 0{\cdot}25\,mm^2$ per each specimen. Fracture toughness was measured by the Vickers indentation technique, which an indentation load of 98 N. The fracture toughness values, K_c, were calculated employing the equation given by Lawn *et al.*[9] A statistical evaluation of the morphology of indentation crack profiles was performed on SEM images. Transmission electron microscopy (TEM) observations were carried out, employing a Philips CM20FEG microscope operating at 200 kV with a point-to-point resolution of 0·24 nm. In order to study the crack paths on the same scale as the triple-grain junctions, TEM foils were also prepared which contained Vickers indentation cracks. Analytical electron microscopy (AEM) was performed by energy-dispersive X-ray spectroscopy (EDX, Tracor, Voyager) with the analytical equipment attached to the microscope. In order to identify the crystalline secondary phases formed upon cooling,

electron diffraction techniques (selected area diffraction (SAD) and microdiffraction) were also employed in addition to the AEM studies.

3 Results and Discussion

Table 1 shows both the grain size and morphology characteristics of the two Si_3N_4 materials investigated. In addition the fracture toughness and the percentage of intergranular fracture path are also given in Table 1. From examining these properties, it can be seen that, although grain size and apparent aspect ratio of the SC_2O_3-doped sample and the $(Al_2O_3+ZrO_2)$-added sample are very similar, the Sc_2O_3-doped Si_3N_4 showed a remarkably higher fracture toughness and a larger percentage of intergranular fracture propagation. This proves that, in the present materials, a further parameter, for example local residual stresses, in addition to the mere Si_3N_4 grain morphology, plays a critical role for determining the fracture behavior. In addition, since the material contains Al, a higher bond strength of a locally formed SiAlON interface has also been proposed.[1]

Some important microstructural characteristics of the two materials were revealed by TEM observations, while imaging the triple-grain junctions. Figure 2 shows a typical crystallized triple pocket in the Sc_2O_3-doped material. The crystalline phase was recognized to be $Sc_2Si_2O_7$ by both EDX and electron diffraction experiments. It is interesting to note that, in this material, devitrification within the triple pockets can proceed up to a volume fraction of crystalline secondary phase close to 100%. Kessler *et al.*[10] have discussed the influence of local internal stresses on the crystallization process of the intergranular phase present at multi-grain junctions in ceramic materials. The outcome of their theoretical analysis showed that according to a strong quadratic dependence of the volume change on the degree of crystallization of glasses, when only low fractions of glass phase crystallize at triple pockets, the volume change is very small. On the other hand, the magnitude of the residual stress built up at triple pockets is proportional to the volume change of the constrained phase. In the present Sc_2O_3-doped material, the nearly 100% fraction of crystallized secondary phase within the pockets implies the presence of significant residual microstresses of tensile nature. Thus, it is expected that a propagating crack tip is driven towards the triple pockets and, when such a pocket is suitably located nearby an acicular Si_3N_4 grain, elastic bridging will occur. On the other hand, when a fine ZrO_2 particle is trapped in a triple pocket with a fixed size which cannot be accommodated by sliding of adjacent interfaces, the positive volume change associated with the martensitic transformation during cooling from the tetragonal phase (stable at high temperature) to the monoclinic structure will cause residual compressive stresses being stored at the triple pockets. Since it is known that the positive volume change in such a transformation is $\approx 5\%$,[11], a local residual stress on the order of GPa can be predicted at ZrO_2 triple pockets. From a micromechanical point of view, the propagating crack tip will deflect its trajectory,

Table 1.

Additives (wt%)	*Grain size (μm)*	*Aspect ratio**	*Intergr. fracture (%)*	*Toughness* $(MPa x\sqrt{m})$
5% Sc_2O_3	0·42	3·3	89	9·6
1·5% Al_2O_3 + 2·7% ZrO_2	0·34	2·8	44	5·1

*Apparent aspect ratio on plane of polish.

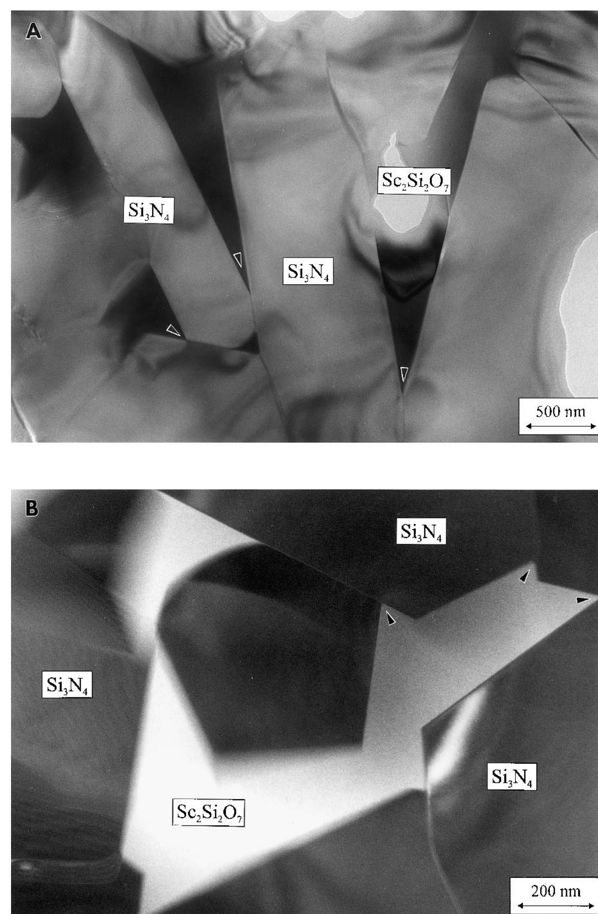

Fig. 2. Elongated grains are observed by TEM in a dark field image of the overall microstructure of the Sc_2O_3-doped Si_3N_4 materials (A). In (B), a higher magnification TEM image of the triple pockets is shown for better clarity. EDX and electron diffraction analyses showed that the triple pockets seen in the micrograph were filled by crystalline $Sc_2Si_2O_7$ phase. Crystallization was found to occur up to the edges of the triple pockets (indicated by arrows in the micrographs).

in order to circumvent the region of the high compressive stress field, resulting in a transgranular propagation through the adjacent grain. A schematic of the interaction between propagating crack and columnar Si_3N_4 grain in the case of highly localized tensile or compressive stresses at triple pockets is shown in Fig. 3(A) and (B), respectively. Microscopy observations indeed proved that debonding along the interface and transgranular crack propagation through the Si_3N_4 grains commonly occur for Sc_2O_3-doped and $(Al_3O_3+ZrO_2)$-doped materials, respectively. Crack profiles for both the materials are shown in Figs 4 and 5. The crystallization of $Sc_3Si_2O_7$ at triple pockets typically favoured intergranular fracture with in some instance even the bifurcation of the crack tip along the interface, as shown in Fig. 4. On the other hand, the effect of the presence of fine ZrO_2 grains at multigrain pockets is that predicted in the presence of high local compressive stresses, namely that a transgranular crack propagation is triggered (Fig. 5). The presence of compressive stresses stored at the Si_3N_4/ZrO_2 interface could be substantiated by TEM imaging, which revealed dark stress contours close to the grain boundaries caused by the local compressive stresses, as shown in Fig. 6 These microscopic characteristics, related to residual microstresses at crystalline triple-grain pockets, can well justify the difference in fracture mode and, accordingly, in fracture toughness, as noticed in these two materials.

Other factors may also affect the fracture mode such as, for example, the different thermal expansion mismatch of the glass caused by different local chemistry of the grain-boundary phase. In addition, due to the presence of Al in the $(Al_2O_3+ZrO_2)$-doped Si_3N_4, it is possible that a layer of SiAlON is formed on the Si_3N_4 grain surface. The local SiAlON formation might significantly alter the intrinsic grain-boundary bonding strength of the material as compared to pure glass. In general, the fracture mode should be

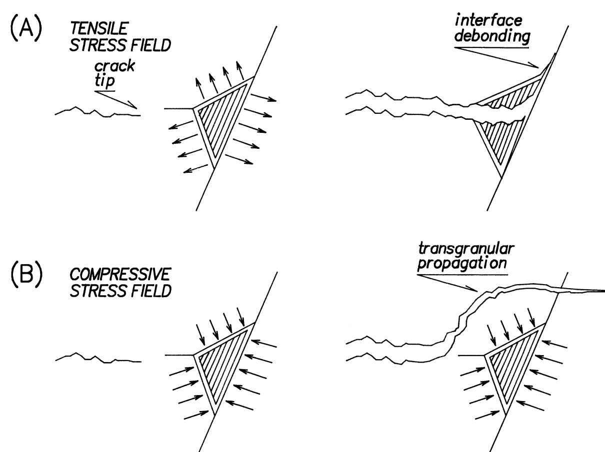

Fig. 3. Schematic of the interaction between propagating crack and columnar Si_3N_4 grain. The cases of highly localized tensile and compressive stresses are shown in (A) and (B), respectively.

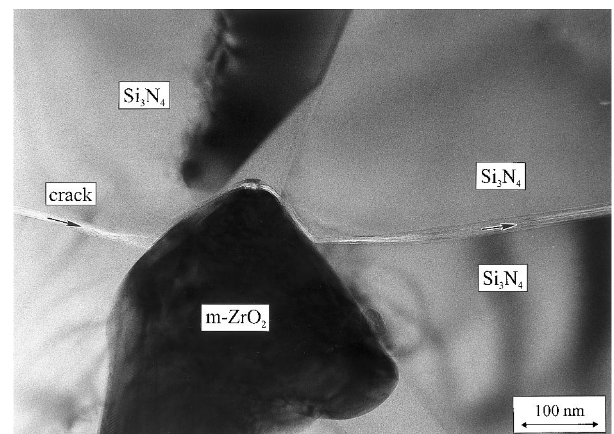

Fig. 5. Interaction of a propagating crack with a triple pocket filled by a fine monoclinic ZrO_2 grain, which was observed by TEM in the $(Al_2O_3+ZrO_2)$-doped Si_3N_4. High local compressive stresses caused transgranular fracture (right hand side) of the adjacent Si_3N_4 grain.

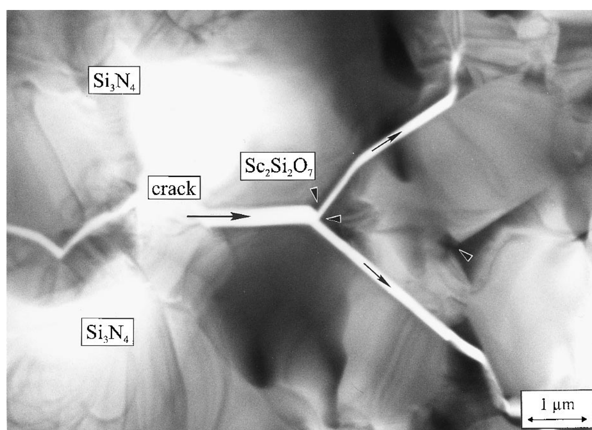

Fig. 4. Splitting of a crack (propagating intergranularly) at a crystallized $Sc_2Si_2O_7$ triple pocket (indicated by arrow) as observed by TEM in the Sc_2O_3-doped Si_3N_4.

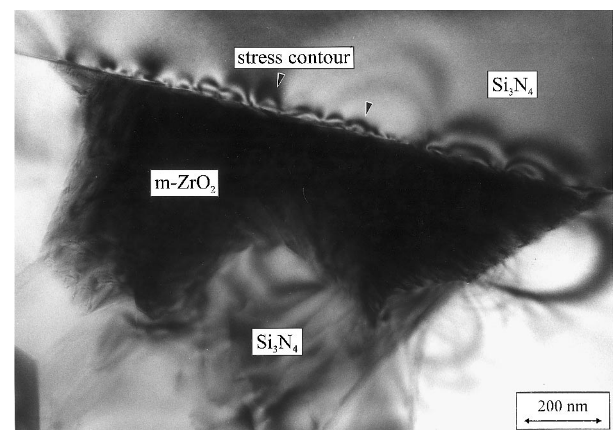

Fig. 6. Bright field TEM image of the m-ZrO_2/Si_3N_4 interface. Bending stress contours are indicated by arrows, which result from the localized high compressive stress at the interface.

determined by a combination of parameters related to both local chemistry and residual stresses at grain boundaries. The microscopy evidences about the influence of local stresses on the fracture mode of Si_3N_4 provided in this paper, should be regarded to hold in particular for the present limit-case materials and to be part of a more general trend including both chemistry and thermal expansion effects. Although evidences for the presence of residual microstresses are only given in a qualitative fashion in this paper, it appears evident that the macroscopic fracture mode and, accordingly, the material toughness, can be controlled by varying the microscopic stress fields at triple pockets.

4 Conclusion

Two limit cases of Si_3N_4 polycrystals with highly compressive or highly tensile residual stress fields at triple pockets were analysed by transmission electron microscopy techniques and tested with respect to fracture toughness. A Si_3N_4 material doped with Sc_2O_3 revealed a tensile stress field localized at triple pockets due to the crystallization of the intergranular glass forming the $Sc_2Si_2O_7$ phase. Such a tensile microstress field promoted intergranular fracture and toughening effect through the formation of elastic bridging sites. On the other hand, a Si_3N_4 material doped with Al_2O_3-ZrO_2 was characterized by highly compressive stress fields at triple pockets due to the martensitic phase transformation (with positive volume change) of small ZrO_2 particles. This material showed a high fraction of transgranular crack propagation and a low toughness, despite the size/morphology of the Si_3N_4 grains was similar to the Sc_2O_3-doped material. TEM observation of the crack path revealed that tensile microstresses trigger intergranular fracture, leading to the formation of bridging sites and, thus, to high toughness.

References

1. Becher, P. F., Hwang, S.-L. and Hsueh, C.-H., Using microstructure to attack the brittle nature of silicon nitride ceramics. *MRS Bull*, 1995, **10**(2), 23–27.
2. Sajgalik, P., Dusza, J. and Hoffmann, M. J., Relationship between microstructure, toughening mechanisms, and fracture toughness of reinforced silicon nitride ceramics. *J. Am. Ceram. Soc.*, 1995, **78**(10), 2619–2624.
3. Choi, S. R., Salem, J. A. and Sanders, W. A., Estimation of crack closure stresses for *in situ* toughened silicon nitride with 8 wt% scandia. *J. Am. Ceram. Soc.*, 1992, **75**(6), 1508–1511.
4. Nishida, T., Hanaki, Y., Nojima, T. and Pezzotti, G., Measurement of rising *R*-curve behavior in toughened silicon nitride by stable crack propagation in bending. *J. Am. Ceram. Soc.*, 1995, **78**(11), 3113–3116.
5. Pezzotti, G., Muraki, N., Maeda, N., Satou, K. and Nishida, T., *In situ* measurement of bridging stresses in toughened Si_3N_4 using raman microprobe spectroscopy. *J. Am. Ceram. Soc.* in press.
6. Bradley, S. A. and Karasek, K. R., Effect of thermal and stress exposure on grain boundaries of silicon nitride. *Ultramicroscopy*, 1989, **29**, 9–17.
7. Pyzik, A. and and Beaman, D. R., Microstructure and properties of self-reinforced silicon nitride. *J. Am. Ceram. Soc.*, 1993, **76**(11), 2727–2744.
8. Peterson, I. M. and Tien, T.-Y., Effect of the grain boundary thermal expansion coefficient on the fracture toughness in silicon nitride. *J. Am. Ceram. Soc.*, 1995, **78**(9), 2345–2352.
9. Lawn, B. R., Evans, A. G. and Marshall, D. B., Elastic/plastic indentation damage in ceramics: the median/radial crack system. *J. Am. Ceram. Soc.*, 1980, **63**(9), 574–581.
10. Kessler, H., Kleebe, H.-J., Cannon, R. W. and Pompe, W., Influence of internal stresses on crystallization of intergranular phases in ceramics. *Acta metall. mater.*, 1992, **40**(9), 2233–2245.
11. Rühle, M., Ma, L. T., Wunderlich, W. and Evans, A. G., TEM studies on phases and phase stabilities of zirconia ceramics. *Physica B*, 1998, **150**, 86–98.